Bayesian Estimation of a Gaussian source in Middleton's Class-A Impulsive Noise

Paolo Banelli, Member, IEEE

arXiv:1111.6828v1 [cs.IT] 29 Nov 2011

Abstract

The paper focuses on minimum mean square error (MMSE) Bayesian estimation for a Gaussian source impaired by additive Middleton's Class-A impulsive noise. In order to reduce the implementation complexity associated with the expression of the optimum Bayesian estimator, the paper considers also two popular suboptimal estimators, which are the soft-limiter and the blanker. The optimum Bayesian thresholds for such suboptimal estimators are obtained by iteratively solving fixed point equations. Connections with the maximum SNR estimators are also established. Theoretical expressions for the MSE and the SNR of the suboptimal estimators are also derived, and the results confirmed by simulations. Noteworthy, the results can be applied to any noise characterized by a Gaussian mixture distribution.

I. INTRODUCTION

INTERFERENCE and noise with impulsive non-Gaussian distributions may impair the performance of several systems including communications, controls, sensors and so forth. Middleton has proposed widely accepted canonical models for interference [1]–[3], which are capable to characterize "intelligent" (e.g., information bearing), as well as "non-intelligent" (e.g., natural or man-made) noises. These models distinguish impulsive interference confined within the observer bandwidth or, equivalently, which does not introduce transitory (i.e., Class-A noise), from wideband interference inducing a transitory in the observing system (i.e., Class-B and Class-C noises) [4]. Although Middleton's noise models were widely investigated to identify the interference behavior [1]–[5], to estimate their canonical parameters [6]–[10], and to detect finite alphabets in digital communications [11]–[16], to the best of the author knowledge, results for the optimum Bayesian estimator (OBE) of Gaussian sources in Class-A impulsive noise are still lacking or, at least, not widely acknowledged. Actually, such OBE estimator would be of valuable help in those applications where the quantity of interest can be modeled, or approximated, by a Gaussian probability density function (*pdf*). This happens, thanks to the central limit theorem (CLT) [17], when the quantity of interest is generated by the superposition of several other non-dominating random quantities.

This is the case, for instance, of a communication system when several signals, possibly belonging to different users, are superimposed in time and multiplexed in another domain, such as the frequency or the code domain. Well know examples are multicarrier systems, such as asymmetric digital subscriber lines (ADSL) [18] and orthogonal frequency division multiplexing (OFDM) [19], or code division multiple access (CDMA) systems [19]. More generally, any multiple-input single-output (MISO) system with a high number of inputs, can be approximately modeled this way.

The first aim of the paper is to derive the minimum mean squared error (MMSE) OBE for a scalar Gaussian source impaired by Middleton's Class-A canonical noise. Noteworthy, such an OBE could be useful also as a preprocessing stage for those estimation and detection algorithms that are designed under AWGN hypotheses and, as such, are not robust to impulsive noises [11], [20]. Although the paper derives the analytical expression of the OBE in a closed form, its use may be restricted in some practical applications due to complexity constraints. In these cases, protection from impulsive noise may be granted by simpler suboptimal devices that are robust to high noise peaks. A possibility is to resort either to a blanking-nonlinearity (BN) that nulls out the received signal when it overpasses a given threshold, or, alternatively, to a soft-limiter (SL) that simply clips the signal when it overpasses the threshold. In both cases, only the blanking or the clipping thresholds have to be optimized in a MMSE Bayesian sense. This way, although both the Bayesian BN estimator (BNE) or the Bayesian SL estimator (SLE) are suboptimal with respect to the OBE, they greatly reduce the implementation complexity, because they only request to store a scalar value (e.g., the threshold), rather than the OBE curve, for the set of source and noise statistical parameters of interest.

Actually, although the SLE and BNE are suboptimal with respect to the OBE, the derivation of the optimum Bayesian thresholds is analytically much harder than the computation of the OBE expression. Specifically, the computation of the optimum thresholds can be formulated in both cases as the solution of a fixed-point problem [21], which is proved to always admit a solution, obtainable by standard iterative approaches with fast convergence.

The comparison of the shape of the OBE curve with the simplified SLE and BNE, can intuitively illuminate whether the BNE or the SLE is the best simplified strategy. The MSE associated to the SLE and the BLE, is the quantitative parameter to choose among the two, and it highlights that the best choice strictly depends on the statistical characteristics of the impulsive noise, which are summarized by the average signal-to-noise power ratio (SNR), the peakness, the average number of emitting noise sources, etc..

A different criterion to set the optimal threshold of a BN, has been proposed in [20], which is based on the maximization of the SNR at the estimator output. The author in [20] exploits an extension of the Bussgang theorem [22], [17] to complex Gaussian mixtures at the input of a nonlinearity (i.e., of the BN). Similar results has been derived also for a SL in a two-component Gaussian mixture noise in [23]. Note that, while MMSE and maximum-SNR (MSNR) are equivalent in pure AWGN scenarios [24], where the MMSE estimator is linear, this is not the case when the noise is a Gaussian-mixture, which leads to a non-linear MMSE estimator. This paper establishes also the connection between the MMSE and the MSNR criteria, at the output of the non-linear estimator. Note that, while [20] and [23] consider a complex Gaussian source, and derive the optimum MSNR thresholds for BN and SL that operate on the complex signal envelope, this paper concentrates on real Gaussian sources impaired by Middleton's Class-A noises. Thus, the optimal MSNR thresholds, derived in this paper for the BN and the SL, are different from those derived in [20] and [23]. If, anyway, the source is a complex Gaussian random variable, the results in this paper can be applied to SL and BN that separately operate on each Cartesian components of the complex source.

Due to the fact that the MMSE and the MSNR approaches are not equivalent, they lead to suboptimal estimators with different thresholds: this paper shows when the two thresholds are similar, and when, conversely, they are different. Whether it is better to maximize the SNR or minimize the MSE, depends on the specific application and design constraint. This is not however the subject of the paper. The paper is organized as follows: section II introduces the system model, while the OBE, SLE, and BNE are derived in sections III, IV, and V, respectively. Successively, section VI establishes the connection between the MMSE and MSNR criteria, and derives the MSE expressions for the SLE and the BNE. Finally section VII is dedicated to computer simulations that confirm the theoretical findings, while the conclusions are drawn in the last section.

II. SYSTEM MODEL

Let's consider a real source x with average power σ_X^2, and zero-mean Gaussian *pdf*, as expressed by

$$f_X(x) = G(x;\sigma_X^2) = \frac{1}{\sqrt{2\pi\sigma_X^2}} e^{-\frac{x^2}{2\sigma_X^2}}, \tag{1}$$

which is impaired by a Class-A impulsive noise n, with average power σ_N^2, as shown in Fig. 1, and summarized by

$$y = x + n. \tag{2}$$

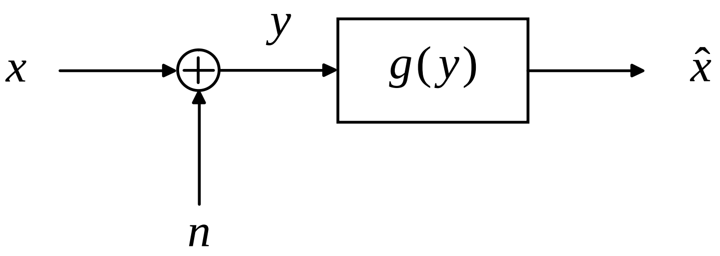

Fig. 1: System model

The Class-A impulsive noise subsumes also the presence of a background zero-mean thermal AWGN n_t, with average power σ_t^2. Specifically, the impulsive noise n has a *pdf* expressed by

$$f_N(n) = \sum_{m=0}^{\infty} \beta_m f_m(n) = \sum_{m=0}^{\infty} \beta_m G(n; \sigma_m^2) = \sum_{m=0}^{\infty} \frac{\beta_m}{\sqrt{2\pi\sigma_m^2}} e^{-\frac{n^2}{2\sigma_m^2}}, \tag{3}$$

which is clearly a Gaussian-mixture, where the weights $\beta_m = e^{-A} A^m / m!$ represent the Poisson-distributed probability that m noise sources simultaneously contribute to the impulsive event [2], [5]. The power σ_m^2 associated with the noise emission from the m noise sources, is expressed by

$$\sigma_m^2 = \frac{m/A + T}{1 + T} \sigma_N^2 = m \frac{\sigma_I^2}{A} + \sigma_t^2, \tag{4}$$

where $\sigma_N^2 = E\{n^2\} = \sigma_I^2 + \sigma_t^2$, σ_I^2 represents the impulsive part of the noise power, $T = \sigma_t^2 / \sigma_I^2$ is the power ratio among the AWGN and the impulsive part of the noise n, and $A = E\{m\} = \sum_{m=0}^{\infty} m\beta_m$ represents the average number of impulsive sources that are simultaneously active. Note that $E\{\cdot\}$ is used throughout the paper for statistical expectation, and $E_X\{\cdot\}$ is used to make explicit that the expectation is computed with respect to the *pdf* of the random variable X.

The overall Class-A model is typically identified by the three canonical parameters, A, T and, σ_N^2, which summarize the statistical structure of the noise. Specifically, low values of A identify rare and highly peaked impulsive sources, and, conversely, high values of A, by a CLT argument, makes the impulsive noise more similar to an AWGN. The interested readers are redirected to [2], [4], [5], and references therein, for further details on the Class-A model, and to [6]–[10], for the estimation of the canonical parameters A, T, and σ_N^2. This paper assumes that the canonical parameters have been perfectly estimated by the observing system.

III. OPTIMUM BAYESIAN ESTIMATOR (OBE)

The optimum non-linear MMSE Bayesian estimator of x given the observed data y, is expressed by [25]

$$\hat{x}_{\text{OBE}}(y) = E_{X|Y}\{x|y\} = \int_{-\infty}^{+\infty} x f_{X|Y}(x;y)dx, \tag{5}$$

where $f_{X|Y}(x;y)$ represents the conditional *pdf* of the source x for a given observation y. By exploiting Bayes rules for conditional *pdf*s, (5) can be expressed as

$$\hat{x}_{\text{OBE}}(y) = \frac{1}{f_Y(y)} \int_{-\infty}^{\infty} x f_{Y|X}\ (y;x)\, f_X(x)dx. \tag{6}$$

Due to the fact that the impulsive noise n is independent of x, it is well known [17] that the probability density function of the observed value y in (2) is given by the linear convolution of the Gaussian *pdf* $f_X(y)$ in (1) with the Middleton-A *pdf* $f_N(y)$ in (3), as expressed by

$$f_Y\,(y) = \sum_{m=0}^{\infty} \beta_m G(y;\sigma_m^2) * G_X(y;\sigma_X^2), \tag{7}$$

where $*$ stands for the linear convolution operator.

Thus, the convolution of two Gaussian *pdf*s generates a new Gaussian *pdf* [17], with variance equal to the sum of the two original variances, and, consequently, equation (7) becomes

$$f_Y\,(y) = \sum_{m=0}^{\infty} \beta_m G(y;\sigma_m^2+\sigma_X^2) = \sum_{m=0}^{\infty} \frac{\beta_m}{\sqrt{2\pi(\sigma_m^2+\sigma_X^2)}} e^{-\frac{y^2}{2\left(\sigma_m^2+\sigma_X^2\right)}}. \tag{8}$$

Observing (2), it is also evident that $f_{Y|X}(y;x)$ in (6), is expressed by

$$f_{Y|X}\,(y;x) = f_N(y-x) = \sum_{m=0}^{\infty} \frac{\beta_m}{\sqrt{2\pi\sigma_m^2}} e^{-\frac{(y-x)^2}{2\sigma_m^2}}. \tag{9}$$

Plugging (9) and (1) in (6), the overall integral becomes

$$\begin{aligned} \hat{x}_{\text{OBE}}(y) &= \tfrac{1}{f_Y(y)} \sum_{m=0}^{\infty} \beta_m \int_{-\infty}^{\infty} x f_X(x) f_m\,(y-x)\,dx \\ &= \tfrac{1}{f_Y(y)} \sum_{m=0}^{\infty} \beta_m\,[p(y) * f_m(y)], \end{aligned} \tag{10}$$

which contains the convolution between the m-th Gaussian *pdf* $f_m(x)$ and $p(x) = x f_X(x)$. The convolution can be computed in the Fourier domain by exploiting the properties of the Fourier transform operator, as detailed in Appendix A, leading to

$$\hat{x}_{\text{OBE}}(y) = \frac{\sum_{m=0}^{\infty} \frac{\sigma_X^2\beta_m}{(\sigma_m^2+\sigma_X^2)^{3/2}} e^{-\frac{y^2}{2(\sigma_m^2+\sigma_X^2)}}}{\sum_{m=0}^{\infty} \frac{\beta_m}{(\sigma_m^2+\sigma_X^2)^{1/2}} e^{-\frac{y^2}{2(\sigma_m^2+\sigma_X^2)}}}\ y. \tag{11}$$

Equation (11) highlights how the OBE depends on the source average power σ_X^2, and the noise canonical parameters A, T, and σ_N^2, through β_m and σ_m^2 in (4). The input-output characteristic of the OBE is plotted in Fig. 2(a) and Fig. 2(b) for several values of the parameter A that controls the peakness of the impulsive noise [5]; it is evident that for very high values of A, when $f_N(n)$ tends to a zero-mean Gaussian *pdf*, the OBE tends to the well known linear-MMSE estimator [25], expressed by

$$\hat{x}_{\text{OBE}}^{(lin)}(y) = \frac{E\{xy\}}{E\{y^2\}} y = \frac{\sigma_X^2}{\sigma_X^2 + \sigma_N^2} y. \tag{12}$$

Conversely, for lower values of A, when the noise is characterizes by rare and highly peaked impulses, the optimum estimator shows a highly non-linear nature, by roughly limiting $(A = 0.1)$ or blanking $(A = 0.001)$ the observed values y that overpass certain thresholds. Note that, the OBE expression in (11), immediately applies also to any other Gaussian-mixture noise n, possibly different from the Class-A noise, with a finite number M of mixtures, such that $\beta_m \geq 0$, and $\sum\limits_{m=0}^{M-1} \beta_m = 1$.

IV. BAYESIAN SOFT LIMITER ESTIMATOR (SLE)

The OBE rather involved analytical expression (11) could prevent its use in real-time applications that are subject to either memory or computational complexity constraints. This is especially true when the OBE analytical expression is requested to be adaptive with respect to changes of either the source or the noise statistical parameters (e.g., the average powers σ_X^2 and σ_N^2, and the noise peakness factors A, and T). For this reason, this section investigates a simple suboptimum estimator, namely the SL estimator shown in Fig. 3, which adds robustness to a system impaired by impulsive noise events, by clipping those values that exceed a given threshold α. Thus, the only parameter to optimize in the Bayesian sense is the clipping threshold α, which obviously would depend on the noise parameters A, T and, σ_N^2, as well as on the source power σ_X^2. Meaningfulness of such an optimization, which leads to the SLE is also suggested by the OBE shapes in Fig. 2(a) and Fig. 2(b), which for certain noise parameters (e.g., $A = 0.1$) resembles the SL estimator of Fig. 3.

Note that, the output of the SL in Fig. 3 is expressed by a non-linear input-output characteristic $\hat{x}_{\text{SL}} = g_{\text{SL}}(y; \alpha)$. Thus, the SL estimation error e_{SL} depends on the selected threshold α, as well as on the statistical properties of the source x and the noise n. This is expressed by

$$e_{\text{SL}} = h_{\text{SL}}(x, n; \alpha) = x - g_{\text{SL}}(x + n; \alpha), \tag{13}$$

where $h_{\text{SL}}(x, n; \alpha)$ highlights that the estimation error e_{SL} is a non linear transformation of two random

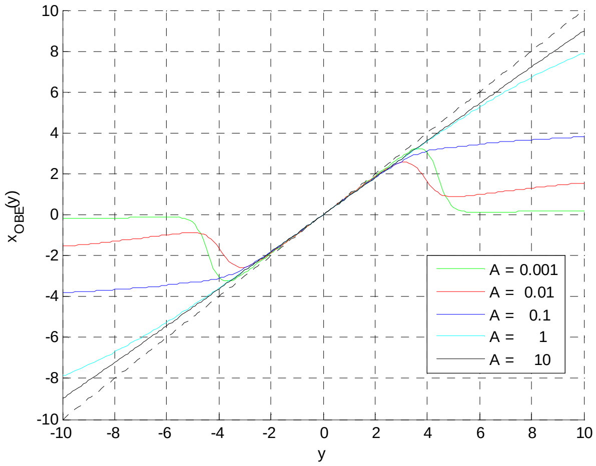

(a) $T = 1$, $\sigma_X^2 = 10$, $\sigma_N^2 = 1$

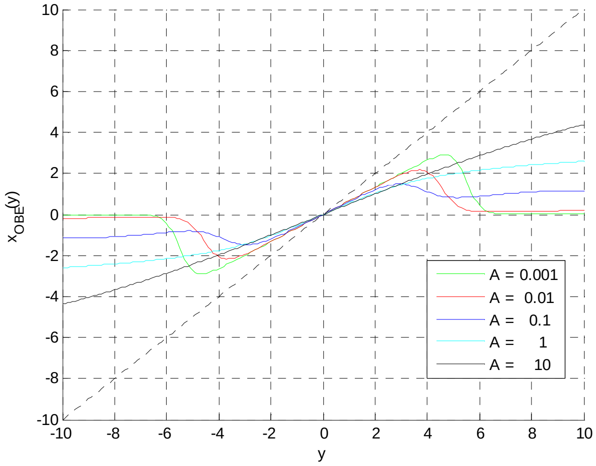

(b) $T = 1$, $\sigma_X^2 = \sigma_N^2 = 1$

Fig. 2: OBE for several values of A

variables, x and n, as summarized by

$$h_{\text{SL}}(x, n; \alpha) = \begin{cases} x + \alpha & , x + n < -\alpha \\ -n & , |x + n| \leq \alpha \\ x - \alpha & , x + n > \alpha \end{cases} . \tag{14}$$

The SLE estimator is defined by selecting $\alpha_{\text{SL}}^{(mse)}$ according to the MMSE criterion, as it follows

$$\alpha_{\text{SL}}^{(mse)} = \underset{\alpha \in \mathcal{R}^+}{\arg\min} \left[E \left\{ e_{\text{SL}}^2 \right\} \right] = \underset{\alpha \in \mathcal{R}^+}{\arg\min} \left[E \left\{ h_{\text{SL}}^2(x, n; \alpha) \right\} \right] . \tag{15}$$

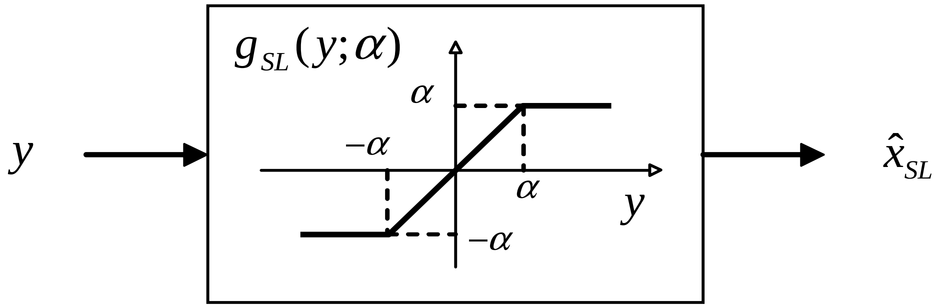

Fig. 3: Soft Limiter estimator

Thus, in order to find $\alpha_{\text{SL}}^{(mse)}$ it is necessary to solve

$$\begin{aligned} \frac{\partial}{\partial\alpha}E\left\{h_{\text{SL}}^2(x,n;\alpha)\right\} &= E\left\{\frac{\partial}{\partial\alpha}\left[h_{\text{SL}}^2(x,n;\alpha)\right]\right\} \\ &= E\left\{2h_{\text{SL}}(x,n;\alpha)h_{\text{SL}}^{(1,\alpha)}(x,n;\alpha)\right\}=0, \end{aligned} \tag{16}$$

where $h_{\text{SL}}^{(1,\alpha)}(x,n;\alpha)$ stands for the first partial derivative of $h_{\text{SL}}(x,n;\alpha)$ with respect to α, and it leads to the following integral equation

$$\int_{-\infty}^{+\infty}\int_{-\infty}^{+\infty} h_{\text{SL}}(x,n;\alpha)h_{\text{SL}}^{(1,\alpha)}(x,n;\alpha)f_X(x)f_N(n)dxdn=0. \tag{17}$$

By substituting (1), (3), (14), and its partial derivative in (17), after tedious derivations detailed in Appendix B, it is proved that $\alpha_{\text{SL}}^{(mse)}$ is the solution of the following fixed-point equation

$$\alpha=F_{\text{SL}}^{(mse)}(\alpha)=2\sigma_X^2\frac{\sum\limits_{m=0}^{\infty}\frac{\beta_m}{\sqrt{2\pi(\sigma_X^2+\sigma_m^2)}}e^{-\alpha^2/2(\sigma_X^2+\sigma_m^2)}}{1-\sum\limits_{m=0}^{\infty}\beta_m\text{erf}\left(\alpha/\sqrt{2(\sigma_X^2+\sigma_m^2)}\right)}. \tag{18}$$

Appendix B proves that the solution of the fixed point equation (18) always exists. Moreover, by conjecturing and proving by simulations that $F_{\text{SL}}^{(mse)}(\alpha)$ is a contraction mapping [21] before its first maximum, it is inferred that the solution is also unique. Thus, the succession $\alpha_{n+1}=F_{\text{SL}}^{(mse)}(\alpha_n)$ converges to the exact fixed point solution $\alpha_{\text{SL}}^{(mse)}$ when n goes to infinity [21]. Consequently, $\alpha_{\text{SL}}^{(mse)}$can be numerically approximated by the following iterative algorithm

A1: Iterative algorithm for optimal SL threshold

```
set $\alpha_0 = F_{\text{SL}}^{(mse)}(0)$ and $n = 0$;
while $|F_{\text{SL}}^{(mse)}(\alpha_n) - \alpha_n| > \varepsilon$ and $n \leq n_{Max}$
    $\alpha_{n+1} = F_{\text{SL}}^{(mse)}(\alpha_n)$ ;
    $n = n + 1$;
end
set $\alpha_{\text{SL}}^{(mse)} = \alpha_n$.
```

In algorithm A1, ε represents the accuracy that is requested for the approximated solution to stop within a maximum number n_{Max} of iterations. Obviously, other iterative numerical approaches can also be used to solve (18), such as the Newton–Rapson method [21] to find the root of $F_{\text{SL}}^{(mse)}(\alpha) - \alpha = 0$.

V. BAYESIAN BLANKING NONLINEARITY ESTIMATOR (BNE)

Fig. 2(a) and Fig. 2(b) suggest that for highly impulsive noise behaviors (e.g., $A = 0.001$), the OBE shape resembles the BN shown in Fig. 4, where the received signal is simply blanked to zero when its absolute magnitude overpasses the threshold α.

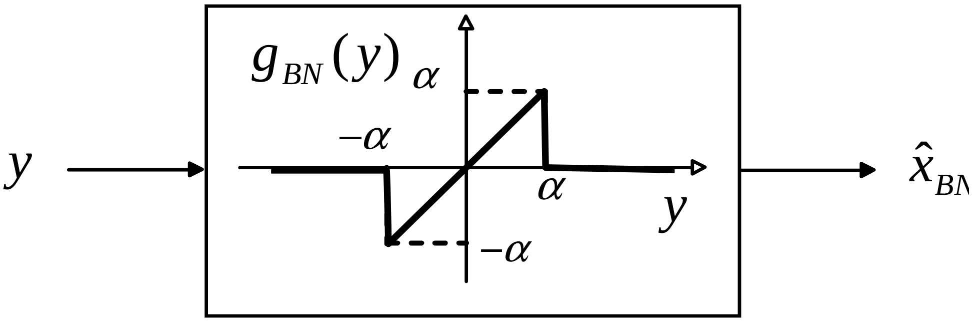

Fig. 4: . Blanking nonlinearity estimator

Similarly to the SLE, the goal is to derive the optimum threshold $\alpha_{\text{BN}}^{(mse)}$ for the BN, in the MMSE sense. In this case the estimation error is

$$e_{\text{BN}} = h_{\text{BN}}(x, n; \alpha) = x - g_{\text{BN}}(x + n; \alpha), \tag{19}$$

where $h_{\text{BN}}(x, n; \alpha)$ is expressed by

$$h_{\text{BN}}(x, n; \alpha) = \begin{cases} -n & , |x+n| \leq \alpha \\ 0 & , |x+n| > \alpha \end{cases} . \tag{20}$$

By derivations similar to those of the SLE, detailed in Appendix C, the optimum $\alpha_{\text{BN}}^{(mse)}$ is given by the solution of the following fixed-point equation

$$\alpha = F_{\text{BN}}^{(mse)}(\alpha) = \frac{\sum\limits_{m=0}^{\infty} \frac{A^m}{m!} \frac{2\sigma_m^2}{(\sigma_X^2+\sigma_m^2)^{3/2}} \alpha e^{-\alpha^2/2(\sigma_X^2+\sigma_m^2)}}{\sum\limits_{m=0}^{\infty} \frac{A^m}{m!} \frac{1}{(\sigma_X^2+\sigma_m^2)^{1/2}} e^{-\alpha^2/2(\sigma_X^2+\sigma_m^2)}} . \tag{21}$$

Although the fixed point problem admits a unique solution, as detailed in Appendix C, $F_{\text{BN}}^{(mse)}(\alpha)$ is not a contraction mapping [21], as it can be observed by Fig. 13. Consequently, $F_{\text{BN}}^{(mse)}(\alpha)$ in (21) is not an attraction for the iterative algorithm A1, and an iterative algorithm that converges to the fixed point is

A2: Iterative algorithm for optimal BN *threshold*

```
set $\alpha_0 > 0,\ 0 < \mu < 1,\ n = 0$;
while $|F_{\text{BN}}^{(mse)}(\alpha_n) - \alpha_n| > \varepsilon$ and $n \leq n_{Max}$
    $\alpha_{n+1} = \alpha_n + \mu(\alpha_n - F_{\text{BN}}^{(mse)}(\alpha_n))$;
    $n = n + 1$;
end
set $\alpha_{\text{BN}}^{(mse)} = \alpha_n$.
```

In algorithm A2, the starting point α_0 has to be greater than zero (for instance $\alpha_0 = 2\sigma_X^2$) to avoid the useless solution $\alpha = 0$, ε represents the accuracy that is requested for the solution within a maximum number of iterations n_{Max}, while μ controls the speed of convergence.

VI. MAXIMUM SNR (MSNR) ESTIMATORS

Any estimator $\hat{x}(y)$ is in general obtained as a non-linear transformation of the observation $y = x + n$. Anyway, it can be always decomposed as a scaled version of the input, plus a distortion term w_y, as expressed by

$$\hat{x} = g(y) = k_y y + w_y, \tag{22}$$

where

$$k_y = E_Y\{\hat{x}y\}/E_Y\{y^2\} \tag{23}$$

is the linear regression coefficient that grants the distortion term is orthogonal to the input term, i.e., $E\{yw_y\} = 0$. In [20], [23] it is suggested to exploit a similar approach to define a MSNR estimator for a complex Gaussian process (an OFDM signal) corrupted by an impulsive Gaussian mixture noise. Note, however, that due to the presence of the impulsive noise n, the non-linearity input $y = x + n$ does not contain only the useful information x.

Thus, in order to define a meaningful SNR [20], it is more convenient to express the estimator output as

$$\hat{x}(y) = g(y) = k_x x + w_x, \tag{24}$$

where

$$k_x = E_{YX}\{g(y)x\}/E_X\{x^2\} = E_{XN}\{g(x+n)x\}/E_X\{x^2\}, \tag{25}$$

is the $partial$ linear regression coefficient that grants the distortion noise w_x is orthogonal to x, as summarized by $E_{XW}\{xw_x\} = 0$. Although in general $k_x \neq k_y$, when the inputs are both zero-mean Gaussian and independent it holds true that $k_x = k_y$ [26]. By this approach, proceeding as suggested in [20], the SNR is expressed by

$$SNR = \frac{k_x^2 E_X\{x^2\}}{E_W\{w^2\}} = \frac{k_x^2 E_X\{x^2\}}{E_{\hat{X}}\{\hat{x}^2\} - k_x^2 E_X\{x^2\}} = \frac{1}{E_Y\{g(y)^2\}/k_x^2\sigma_X^2 - 1}, \tag{26}$$

where the second equality in (26) is granted by the uncorrelation between the useful part and the distortion noise. Clearly, the optimum non-linear estimator, in the maximum SNR sense, is expressed by

$$\hat{x}_{SNR}(y) = \underset{g(y)}{\arg\max}\,[SNR] = \underset{g(y)}{\arg\min}\left[E_Y\{g(y)^2\}/E_{XY}^2\{g(y)x\}\right]. \tag{27}$$

In the problem at hand, taking into account that n is distributed according to (3), the computation of k_x in the denominator of (26) and (27), can be obtained by

$$k_x = \frac{E_{XN}\{g(x+n)x\}}{\sigma_X^2} = \sum_{m=0}^{\infty} \beta_m \frac{E_{XN_m}\{g(x+n)x\}}{\sigma_X^2}, \tag{28}$$

where the subscript N_m means that the expected value is computed with respect to the m-th Gaussian *pdf* $G(n;\sigma_m^2)$ associated to the Class-A Gaussian mixture. This fact suggests that the constant k_x can be expressed as the weighted sum of other constants

$$k_{x,m} = \frac{E_{XN_m}\{g(x+n_m)x\}}{\sigma_X^2}, \tag{29}$$

which can be interpreted as the gain associated to the (*virtual*) useful components at the output of the non-linear estimator, when it is separately driven by the (*virtual*) input $y_m = x + n_m$. Note that, each *virtual* input y_m is the sum of two zero-mean independent Gaussian random variables, thus, it is also zero-mean Gaussian distributed with variance $\sigma_{y,m}^2 = \sigma_X^2 + \sigma_m^2$.

In this virtual set-up, (see Theorem 1 in [26]), it holds true that

$$k_{x,m} = \frac{E_{XN_m}\{g(x+n_m)x\}}{\sigma_X^2} = k_{y,m} = \frac{E_{Y_m}\{g(y_m)y_m\}}{\sigma_{y,m}^2}, \tag{30}$$

where the expectation on the right-hand side of (30) involves a single-folded integral, which is much simpler to compute than the two-folded integral in its left-hand side. Moreover, last equality in (30) is attractive because it is possible to exploit widely known results for the output of several non-linear devices (such as the BN and the SL) driven by Gaussian inputs [22], [27]–[30].

Similarly, it is straightforward to derive that the average estimator output power, in the numerator of (27), can be expressed as

$$P_{\hat{X}} = E_Y\{g(y)^2\} = \sum_{m=0}^{\infty} \beta_m E_{Y_m}\{g^2(y_m)\}, \tag{31}$$

where also right-hand side of (31) can exploit results widely available in the said technical literature for non-linear devices driven by Gaussian inputs.

However, despite the above simplifications, the solution of the functional optimization problem in (27) is not easy, and consequently the derivation of the optimum estimator in the MSNR sense, is still an open problem. Conversely, it is possible to exploit (30) and (31), if $g(y)$ is constrained to belong to families of suboptimal estimators,

$$\hat{x}_{\mathrm{XX}}(y) = g_{\mathrm{XX}}(y;\alpha), \tag{32}$$

where XX stands for either the SL or the BN, and α is a scalar parameter that univocally specifies $g_{\mathrm{XX}}(\cdot,\alpha)$. In this case the problem reduces to a classical optimization with respect to the scalar parameter α, where the optimum thresholds in the MSNR sense, for either the SL or the BN, are expressed by

$$\alpha_{\mathrm{XX}}^{(snr)} = \arg\min_{\alpha\in\mathcal{R}^+} \left[E_Y\{\hat{x}_{\mathrm{XX}}^2(y)\}/(k_x^{(\mathrm{XX})})^2\right]. \tag{33}$$

Thus, taking into account that the logarithm is a monotonic function, i.e., it does not change the position of extreme values, the optimum $\alpha_{\mathrm{XX}}^{(snr)}$ can be obtained by solving

$$\frac{\partial}{\partial\alpha}\left\{\log\frac{E_Y\{\hat{x}_{\mathrm{XX}}^2(y)\}}{(k_x^{(\mathrm{XX})})^2}\right\} = 0, \tag{34}$$

which leads to

$$\frac{1}{E_Y\{\hat{x}_{\mathrm{XX}}^2(y)\}}\frac{\partial}{\partial\alpha}E_Y\{\hat{x}_{\mathrm{XX}}^2(y)\} - \frac{2}{k_x^{(\mathrm{XX})}}\frac{\partial}{\partial\alpha}k_x^{(\mathrm{XX})} = 0. \tag{35}$$

When the non linear device is the SL $g_{\text{SL}}(y;\alpha)$ of Fig. 3, it is straightforward to derive [22] that

$$k_m^{(\text{SL})} = \frac{E_{Y_m}\{g_{\text{SL}}(y_m;\alpha)y_m\}}{\sigma_{y,m}^2} = \text{erf}\left(\frac{\alpha}{\sqrt{2}\sigma_{y,m}}\right), \tag{36}$$

and, consequently,

$$k_x^{(\text{SL})} = \sum_{m=0}^{\infty} \beta_m \text{erf}\left(\frac{\alpha}{\sqrt{2(\sigma_X^2+\sigma_m^2)}}\right), \tag{37}$$

where the error function is defined as $\text{erf}(x) = (2/\sqrt{\pi})\int_0^x e^{-t^2}dt$. Analogously, when the non-linear estimator is the BN $g_{\text{BN}}(y;\alpha)$ of Fig. 4, by standard integration techniques it is possible to prove that

$$k_m^{(\text{BN})} = \frac{E_{Y_m}\{g_{\text{BN}}(y_m;\alpha)y_m\}}{\sigma_{y,m}^2} = k_m^{(\text{SL})} - \frac{2}{\sqrt{\pi}}\frac{\alpha}{\sigma_{y,m}}e^{-\frac{\alpha^2}{2\sigma_{y,m}^2}}, \tag{38}$$

and, consequently,

$$k_x^{(\text{BN})} = k_x^{(\text{SL})} - \frac{2}{\sqrt{\pi}}\sum_{m=0}^{\infty}\beta_m\frac{\alpha}{\sigma_{y,m}}e^{-\frac{\alpha^2}{2(\sigma_X^2+\sigma_m^2)}}. \tag{39}$$

Similarly, plugging $g_{\text{SL}}(y;\alpha)$ and $g_{\text{BN}}(y;\alpha)$ in (31), by standard integration techniques for Gaussian *pdf*s, it is straightforward to derive

$$E_Y\{\hat{x}_{\text{BN}}^2(y)\} = \sum_{m=0}^{\infty}\beta_m\sigma_{y,m}^2\left[\text{erf}\left(\frac{\alpha}{\sqrt{2}\sigma_{y,m}}\right) - \sqrt{\frac{2}{\pi}}\frac{\alpha}{\sigma_{y,m}}e^{-\frac{\alpha^2}{2\sigma_{y,m}^2}}\right] \tag{40}$$

and

$$E_Y\{\hat{x}_{\text{SL}}^2(y)\} = E_Y\{\hat{x}_{\text{BN}}^2(y)\} + \alpha^2\sum_{m=0}^{\infty}\beta_m\left[1-\text{erf}\left(\frac{\alpha}{\sqrt{2}\sigma_{y,m}}\right)\right]. \tag{41}$$

Note that (37), (39), (40) and (41) are different from the corresponding equations in [20], [23], because this paper deals with SL and BN of real random variables, while [20] and [23] consider the SL and the BN of the envelope of complex random variables. However, if the source is a complex Gaussian random variable, (37), (39), (40), and (41) can be applied to SL and BN that separately operate on each Cartesian component of the complex source.

Plugging (38) and (40) in (35), after standard algebraic manipulation the optimal BN threshold $\alpha_{\text{BN}}^{(snr)}$ is the solution of the following equation

$$\frac{\sum_{m=0}^{\infty}\frac{\beta_m}{\sqrt{2}\sigma_{y,m}}e^{-\alpha^2/2\sigma_{y,m}^2}}{E\left\{\hat{x}_{\text{BN}}^2(y)\right\}} - \frac{\sum_{m=0}^{\infty}\frac{\sqrt{2}\beta_m}{\sigma_{y,m}^3}e^{-\alpha^2/2\sigma_{y,m}^2}}{k_x^{(\text{BN})}} = 0. \tag{42}$$

Analogously, plugging (37) and (41) in (35), the optimal SL threshold $\alpha_{\text{SL}}^{(snr)}$ is the solution of the following equation

$$\frac{\sum_{m=0}^{\infty}\alpha\beta_m\left(1-\text{erf}\left(\frac{\alpha}{\sqrt{2}\sigma_{y,m}}\right)\right)}{E\left\{\hat{x}_{\text{SL}}^2(y)\right\}} - \frac{\sqrt{\frac{2}{\pi}}\sum_{m=0}^{\infty}\frac{\beta_m}{\sigma_{y,m}}e^{-\alpha^2/2\sigma_{y,m}^2}}{k_x^{(\text{SL})}} = 0. \tag{43}$$

Note that while (42) has to be solved by root-finding numerical techniques [21], (43) could also be solved by iterative numerical approaches similar to A1 and A2, by exploiting its equivalent fixed-point formulation

$$\alpha = F_{\text{SL}}^{(snr)}(\alpha) = \frac{E\left\{\hat{x}^2_{\text{SL}}(y)\right\}}{k_x^{(\text{SL})}} \cdot \frac{\sqrt{\frac{2}{\pi}} \sum\limits_{m=0}^{\infty} \frac{\beta_m}{\sigma_{y,m}} e^{-\alpha^2/2\sigma^2_{y,m}}}{1 - \sum\limits_{m=0}^{\infty} \beta_m \text{erf}\left(\frac{\alpha}{\sqrt{2}\sigma_{y,m}}\right)}. \tag{44}$$

It is interesting to observe that the fixed-point problem in (44) can be expressed as

$$\alpha = F_{\text{SL}}^{(snr)}(\alpha) = \frac{E\left\{\hat{x}^2_{\text{SL}}(y)\right\}}{\sigma^2_X k_x^{(\text{SL})}} \cdot F_{\text{SL}}^{(mse)}(\alpha), \tag{45}$$

which highlights that the fixed-point MSNR solution is in general different from the MMSE solution in (18). However, when the optimal thresholds are sufficiently higher than the input standard deviation σ_y, the power of the distortion noise is quite low and $E\{\hat{x}^2_{SL}\} \approx k_x^2 \sigma_X^2$, and, by (45), the two optimal thresholds are very close if $k_x \approx 1$. This fact can be further appreciated, by observing that the optimal MMSE thresholds are obtained by

$$\alpha_{\text{XX}}^{(mse)} = \underset{\alpha \in \mathcal{R}^+}{\arg\min} \left[E_e\{e^2\}\right], \tag{46}$$

and that, according to (24), the estimation error can also be expressed as

$$e = x - \hat{x}(y) = (1 - k_x)x - w_x. \tag{47}$$

Thus, exploiting the orthogonality between x and w_x, an alternative expression for the MSE is

$$E_E\{e^2\} = (1 - k_x)^2 \sigma_X^2 + E_{W_x}\{w_x^2\}, \tag{48}$$

and, exploiting$E_Y\{\hat{x}^2_{\text{XX}}(y)\} = \left[k_x^{(\text{XX})}\right]^2 \sigma_X^2 + E_{W_x}\{w_x^2\}$, it is possible to conclude that

$$E_E\{e^2\} = (1 - 2k_x^{(\text{XX})})\sigma_X^2 + E_Y\{\hat{x}^2_{\text{XX}}(y)\}. \tag{49}$$

This means that the MSE optimal threshold is obtained by

$$\begin{aligned}
\alpha_{\text{XX}}^{(mse)} &= \underset{\alpha \in \mathcal{R}^+}{\arg\min} \left[E_Y\{\hat{x}^2_{\text{XX}}(y)\} - 2k_x^{(\text{XX})}\sigma_X^2\right] \\
&= \underset{\alpha \in \mathcal{R}^+}{\arg\min} \left[E_Y\{\hat{x}^2_{\text{XX}}(y)\}/k_x^{(\text{XX})} - 2\sigma_X^2\right] \\
&= \underset{\alpha \in \mathcal{R}^+}{\arg\min} \left[E_Y\{\hat{x}^2_{\text{XX}}(y)\}/k_x^{(\text{XX})}\right] \\
&= \underset{\alpha \in \mathcal{R}^+}{\arg\min} \left[\left((k_x^{(\text{XX})})^2\sigma_X^2 + \sigma_{W_x}^2\right)\Big/k_x^{(\text{XX})}\right],
\end{aligned} \tag{50}$$

which is different from the MSNR criterion in (33) due to the absence of the square-power in the denominator of the cost function. Thus, MMSE and MSNR approaches provide very close thresholds when $k_x^{(\mathrm{XX})} \approx 1$, which happens, for instance, when the clipping threshold α is sufficiently higher than σ_y, due to $\sigma_N^2 \ll \sigma_X^2$ (see also (12)).

Noteworthy, the alternative expression (49) is very useful for the computation of the MSE, because it requests to compute only single-folded integrals, i.e., the estimator average output power $E_Y\{\hat{x}^2_{\mathrm{XX}}(y)\}$ by (31) (i.e., (40) and (41), for BNE and SLE) and the gain $k_x^{(\mathrm{XX})}$ by (28) (i.e., (38) and (39), for BNE and SLE). Conversely, according to (13) or (19), the MSE should be computed by

$$E_E\{e^2\} = E_{XN}\{h^2(x,n;\alpha)\} = \sum_{m=0}^{\infty} \beta_m E_{XN_m}\{h^2(x,n_m;\alpha)\}, \qquad (51)$$

which involves tedious double-folded integrals with respect to the signal and the noise *pdf*s.

VII. COMPUTER SIMULATIONS

This section verifies by computer simulations the analytical results derived so far. The MSE and SNR performance of the SL and BN are computed for several sets of the Class-A canonical parameters A, T, σ_N^2 and for several SNR values. All the simulated MSE and SNR are obtained by generating 10^8 observed samples y in (2). The Middleton's Class-A noise has been generated by the toolbox [31]. The optimal thresholds for the MMSE SL and BN are obtained by A1 and A2, using $\varepsilon = 0.01$ and $\mu = 0.01$. The thresholds for the MSNR SL and BN are obtained by Matlab® numerical solutions of (43) and (42), respectively. The series with infinite terms, which are induced in all the analytical results by the Class-A *pdf* in (3), have been approximated by considering only the first $M = 50$ terms (although, $M \in [10, 20]$ would be enough in most of the cases).

It is possible to observe in Fig. 5 and Fig. 6, the dependence of the optimal SL and BN thresholds on the total SNR, which is defined as $SNR_{tot} = \sigma_X^2/(\sigma_t^2 + \sigma_I^2)$. It is shown that the MMSE and MSNR (optimal) thresholds are similar for high values of SNR_{tot} (i.e., when $\sigma_X^2 \gg \sigma_N^2$), where, consequently, the two criterion are almost equivalent. This is not the case, for low (and negative) values of the SNR_{tot}, where the MMSE and MSNR thresholds tend to diverge. Moreover, it is to note that the MMSE and MSNR thresholds tend to be more different for the BN rather than for the SL. This fact is more evident when $T = \sigma_t^2/\sigma_I^2 = 1$, i.e., when the noise power is equally split between the AWGN and the impulsive component.

Fig. 7-Fig. 12 let to better appreciate the sensitiveness of the SNR and MSE performance with respect to the thresholds values of both the SL and the BN, and their performance penalties with respect to the OBE. Note that in all the figures the minimum MSE and the maximum SNR, correspond exactly to the thresholds values predicted by the theory. Moreover, also the theoretical MSE and SNR, perfectly match with simulation results. As already anticipated, in most of the scenarios the optimal MMSE and MSNR thresholds are almost equivalent, and consequently they provide almost the same MSE and SNR performance. This is not the case however, in highly critical scenarios, when the SNR_{tot} is quite low or negative, and the AWGN noise power is not negligible, with respect to the impulsive noise power (either because $T \approx 1$ or because the impulsive noise tends to a Gaussian noise when $A \approx 1$). All the figures also highlight that the OBE, as theoretically expected, always outperforms the SL and the BN in MSE. The SL and BN penalties however are not dramatic, as it was expected by the fact that the OBE shapes in Fig. 2(a) highly resemble either the SL or the BN, for several values of the canonical Class-A parameters. Interestingly the OBE derived in this paper, although it is not the MSNR optimal estimator, it outperforms in SNR the MSNR (sub-) optimal BN and SL, in most of the cases.

CONCLUSIONS

This paper has derived the MMSE Bayesian estimator for a Gaussian source impaired by impulsive Middleton's Class-A interference. The estimator is directly extensible to any Gaussian-mixture noise. Two popular and sub-optimal estimators, namely the soft-limiter and the blanker, have been optimized both in a MSE and SNR sense, deriving also closed form expressions for their MSE and SNR. A theoretical link between MSE and SNR at the output of the estimator has been established, and scenarios when the MMSE and the maximum SNR criteria are (almost) equivalent, or different, have been clarified. The theoretical analysis and computer simulations have shown that at least one estimator, among the optimum soft-limiter or the optimum blanker, can be always used as a sub-optimum estimator with minimal performance loss with respect to the MMSE Bayesian estimator. The derivation of the optimal estimator in the maximum-SNR sense, as well as a closed-form expression for the MSE of the optimal Bayesian estimator, are still open problems for possible further research.

APPENDIX A

OBE DERIVATION

$S(f) = \mathcal{F}\{s(x)\}$ is used to indicate the Fourier transform (FT) of $s(x)$, defined by $\mathcal{F}\{s(x)\} = \int\limits_{-\infty}^{+\infty} s(x)e^{-j2\pi fx}dx$. It is also reminded that the FT of a Gaussian *pdf* is still a normalized Gaussian function, as expressed by

$$\mathcal{F}\{G(x;\sigma_X^2)\} = \tilde{G}(f;\sigma_{X,f}^2) = G(f;\sigma_{X,f}^2)/G(0;\sigma_{X,f}^2), \tag{52}$$

where $\sigma_{X,f}^2 = 1/(4\pi\sigma_X^2)$. Thus, by exploiting the convolution and derivative properties of the FT transform, the integral in (10) can be expressed in the frequency domain by

$$\begin{aligned} \mathcal{F}\{p_x(x) * f_m(x)\} &= \mathcal{F}\{p_x(x)\}\,\mathcal{F}\{f_m(x)\} \\ &= \mathcal{F}\{xG(x;\sigma_X^2)\}\,\mathcal{F}\{G(x;\sigma_m^2)\} \\ &= \tfrac{j}{2\pi}\tfrac{d}{df}\left[\tilde{G}(f;\sigma_{X,f}^2)\right]\tilde{G}(f;\sigma_{m,f}^2). \end{aligned} \tag{53}$$

By observing that the first derivative of a Gaussian function is expressed by

$$\frac{d}{df}\left[G(f;\sigma^2)\right] = -\frac{f}{\sigma^2}G(f;\sigma^2), \tag{54}$$

then (53) becomes

$$\mathcal{F}\{p_x(x) * f_m(x)\} = -\frac{j}{2\pi\sigma_{X,f}^2} f\ \tilde{G}(f;\sigma_{X,f}^2)\tilde{G}(f;\sigma_{m,f}^2). \tag{55}$$

Thus, by the duality property of the inverse FT

$$\begin{aligned} p_x(x) * f_m(x) &= -\tfrac{j}{2\pi\sigma_{X,f}^2}\mathcal{F}^{-1}\left\{f\ \tilde{G}(f;\sigma_{X,f}^2)\tilde{G}(f;\sigma_{m,f}^2)\right\} \\ &= -\tfrac{1}{4\pi^2\sigma_{X,f}^2}\tfrac{d}{dx}\left[\mathcal{F}^{-1}\left\{\tilde{G}(f;\sigma_{X,f}^2)\tilde{G}(f;\sigma_{m,f}^2)\right\}\right] \\ &= -\sigma_X^2\tfrac{d}{dx}\left[G(x;\sigma_X^2) * G(x;\sigma_m^2)\right]. \end{aligned}$$

Exploiting the well known property that the convolution of zero-mean Gaussian $pdfs$ is still a zero-mean Gaussian *pdf*, with a variance equal to the sum of the two single variances

$$p_x(x) * f_m(x) = -\sigma_X^2\frac{d}{dx}G(x;\sigma_X^2+\sigma_m^2) = \frac{\sigma_X^2}{\sigma_X^2+\sigma_m^2}xG(x;\sigma_X^2+\sigma_m^2). \tag{56}$$

Summarizing, equation (10) can be expressed by

$$\hat{x}_{\text{OBE}}(y) = \frac{1}{f_Y(y)}\sum_{m=0}^{\infty}\beta_m\left[p(y) * f_m(y)\right] = \frac{\sum\limits_{m=0}^{\infty}\frac{\sigma_X^2\beta_m}{\sigma_X^2+\sigma_m^2}G(y;\sigma_X^2+\sigma_m^2)}{\sum\limits_{m=0}^{\infty}\beta_m G(y;\sigma_X^2+\sigma_m^2)}y, \tag{57}$$

which coincides with (11).

APPENDIX B

SLE DERIVATION

By observing (14) it is clear that $h_{\mathrm{SL}}(x,n;\alpha)$ is continuous with respect to $\alpha \in \mathcal{R}^+$ and that

$$h_{\mathrm{SL}}(x,n;\alpha)h_{\mathrm{SL}}^{(1,\alpha)}(x,n;\alpha) = \begin{cases} x+\alpha & ,x < -\alpha - n \\ 0 & ,|x+n| \le \alpha \\ \alpha - x & ,x > -n+\alpha \end{cases} . \tag{58}$$

Consequently, substituting (58) in (16), the optimum value $\alpha_{SLE}^{(mse)}$ is obtained by the solution of the following equation

$$\int\limits_{-\infty}^{+\infty}\int\limits_{-\infty}^{-\alpha-n}(x+\alpha)f_X(x)dxf_N(n)dn + \int\limits_{-\infty}^{+\infty}\int\limits_{\alpha-n}^{+\infty}(\alpha-x)f_X(x)dxf_N(n)dn = 0, \tag{59}$$

which, by standard integration of Gaussian density functions, is equivalent to

$$\alpha = \frac{N_{\mathrm{SL}}(\alpha)}{D_{\mathrm{SL}}(\alpha)} = \frac{\frac{\sigma_X}{\sqrt{2\pi}}\int\limits_{-\infty}^{+\infty}\left[e^{-(\alpha+n)^2/2\sigma_X^2} + e^{-(\alpha-n)^2/2\sigma_X^2}\right]f_N(n)dn}{\int\limits_{-\infty}^{+\infty}\left[\Phi\left(-\frac{n+\alpha}{\sigma_X}\right)+\Phi\left(\frac{n-\alpha}{\sigma_X}\right)\right]f_N(n)dn}, \tag{60}$$

where $\Phi(x) = 0.5\left[1+\mathrm{erf}\left(x/\sqrt{2}\right)\right]$.

By substituting in (60) the expression of $f_N(n)$ in (3), it is recognized, by means of (1), that the numerator

$$N_{\mathrm{SL}}(\alpha) = \sigma_X^2 e^{-A}\sum_{m=0}^{\infty}\frac{A^m}{m!}\left[\int\limits_{-\infty}^{+\infty}G(n;\sigma_m^2)G(\alpha-n;\sigma_X^2)dn + \int\limits_{-\infty}^{+\infty}G(n;\sigma_m^2)G(\alpha+n;\sigma_X^2)dn\right], \tag{61}$$

contains two integrals that represent the convolution, and the correlation, of two zero-mean Gaussian $pdfs$. Due to the even symmetry of Gaussian functions, the correlation is equivalent to the convolution, and the result is another zero-mean Gaussian *pdf*, with a variance equal to the sum of the two single variances, as expressed by

$$\begin{aligned} N_{\mathrm{SL}}(\alpha) &= 2\sigma_X^2\sum_{m=0}^{\infty}\beta_m G(\alpha;\sigma_X^2+\sigma_m^2) = 2\sigma_X^2\sum_{m=0}^{\infty}e^{-A}\frac{A^m}{m!}\frac{e^{-\alpha^2/2(\sigma_X^2+\sigma_m^2)}}{\sqrt{2\pi(\sigma_X^2+\sigma_m^2)}} \\ &= 2\sigma_X^2\sum_{m=0}^{\infty}N_m(\alpha). \end{aligned} \tag{62}$$

As far as the denominator $D_{\mathrm{SL}}(\alpha)$ in (60), it is possible to recognize that

$$D_{\mathrm{SL}}(\alpha) = e^{-A}\sum_{m=0}^{\infty}\frac{A^m}{m!}\int\limits_{-\infty}^{+\infty}\left[\Phi\left(\frac{-n-\alpha}{\sigma_X}\right)+\Phi\left(\frac{n-\alpha}{\sigma_X}\right)\right]G(n;\sigma_m^2)dn,$$

which can be rewritten as

$$D_{\mathrm{SL}}(\alpha) = 1 + \frac{e^{-A}}{2}\sum_{m=0}^{\infty}\frac{A^m}{m!}\int\limits_{-\infty}^{+\infty}\left[-\mathrm{erf}\left(\frac{n+\alpha}{\sigma_X}\right)+\mathrm{erf}\left(\frac{n-\alpha}{\sigma_X}\right)\right]G(n;\sigma_m^2)dn.$$

Exploiting the odd and even symmetry properties of $\mathrm{erf}(\cdot)$ and $G(\cdot;\sigma^2)$, respectively, and by a change of integration variable, it is finally obtained

$$\begin{array}{rcl} D_{\mathrm{SL}}(\alpha) & = & 1+e^{-A}\sum\limits_{m=0}^{\infty}\frac{A^m}{m!}\frac{\sigma_X}{\sqrt{\pi}\sigma_m}\int\limits_{-\infty}^{+\infty}e^{-(\sqrt{2}\sigma_X z+\alpha)^2/2\sigma_m^2}\mathrm{erf}\left(z\right)dz \\ & = & 1+e^{-A}\sum\limits_{m=0}^{\infty}\frac{A^m}{m!}\frac{\sigma_X}{\sqrt{\pi}\sigma_m}e^{-\alpha^2/2\sigma_m^2}\int\limits_{-\infty}^{+\infty}e^{-pz}e^{-bz^2}\mathrm{erf}\left(z\right)dz \end{array}, \qquad (63)$$

where $p=\sqrt{2}\alpha\sigma_X/\sigma_m^2$, and $b=\sigma_X^2/\sigma_m^2$. The last integral in (63) can be rearranged as follows

$$\int\limits_{-\infty}^{+\infty}e^{-pz}e^{-bz^2}\mathrm{erf}\left(z\right)dz=\int\limits_{-\infty}^{0}e^{-pz}e^{-bz^2}\mathrm{erf}\left(z\right)dz+\int\limits_{0}^{\infty}e^{-pz}e^{-bz^2}\mathrm{erf}\left(z\right)dz,$$

which, by inverting the integration variable in the first term, turns to be equal to

$$\int\limits_{-\infty}^{+\infty}e^{-bz^2}\mathrm{erf}\left(z\right)\left[e^{-pz}-e^{pz}\right]dz=-2\int\limits_{-\infty}^{+\infty}e^{-bz^2}\mathrm{erf}\left(z\right)\sinh(pz)dz.$$

Substituting (64) in (63), and exploiting 2.8.10.2 in [32], vol. 2, pag. 111], it is finally obtained

$$\begin{array}{rcl} D_{\mathrm{SL}}(\alpha) & = & 1-e^{-A}\sum\limits_{m=0}^{\infty}\frac{A^m}{m!}\frac{\sigma_X}{\sqrt{\pi}\sigma_m}e^{-\alpha^2/2\sigma_m^2}\sqrt{\frac{\pi}{b}}e^{\frac{p^2}{4b}}\mathrm{erf}\left(\frac{p}{2\sqrt{b+b^2}}\right) \\ & = & 1-e^{-A}\sum\limits_{m=0}^{\infty}\frac{A^m}{m!}\mathrm{erf}\left(\frac{\alpha}{\sqrt{2(\sigma_m^2+\sigma_X^2)}}\right). \end{array}$$

In order to prove the existence and the uniqueness of the solution to the fixed point equation (18), note that the relative minima and maxima of $F_{\mathrm{SL}}^{(mse)}(\alpha)$, are associated to the zeros of $F_{\mathrm{SL}}^{(1,\alpha)}(\alpha)=dF_{\mathrm{SL}}^{(mse)}(\alpha)\Big/d\alpha$, expressed by

$$\begin{array}{rcl} F_{\mathrm{SL}}^{(1,\alpha)}(\alpha) & = & \frac{2\sigma_X^2}{D_{\mathrm{SL}}(\alpha)^2}\left[-\sum\limits_{m=0}^{\infty}\frac{\alpha}{\sigma_X^2+\sigma_m^2}N_m(\alpha)D_{\mathrm{SL}}(\alpha)+\sum\limits_{m=0}^{\infty}\frac{2\beta_m}{\sqrt{2\pi(\sigma_X^2+\sigma_m^2)}}N_m(a)N_{\mathrm{SL}}(\alpha)\right] \\ & = & 4\sigma_X^2\frac{N_{\mathrm{SL}}(\alpha)^2}{D_{\mathrm{SL}}(\alpha)^2}-\frac{2\alpha}{D_{\mathrm{SL}}(\alpha)}\sum\limits_{m=0}^{\infty}\frac{\sigma_X^2}{\sigma_X^2+\sigma_m^2}N_m(a). \end{array} \qquad (64)$$

Thus, the relative minima and maxima, correspond to values α^* that satisfy the following expression

$$\alpha^*=\frac{2\sigma_X^2}{\sum\limits_{m=0}^{\infty}\frac{\sigma_X^2}{\sigma_X^2+\sigma_m^2}N_m(\alpha^*)}\frac{N_{\mathrm{SL}}^2(\alpha^*)}{D_{\mathrm{SL}}(\alpha^*)}=F_{\mathrm{SL}}^{(mse)}(\alpha^*)\frac{\sum\limits_{m=0}^{\infty}N_m(\alpha^*)}{\sum\limits_{m=0}^{\infty}\frac{\sigma_X^2}{\sigma_X^2+\sigma_m^2}N_m(\alpha^*)}>F_{\mathrm{SL}}^{(mse)}(\alpha^*). \qquad (65)$$

Taking in mind that $F_{\mathrm{SL}}^{(mse)}(0)=N_{\mathrm{SL}}(0)>0$ and $F_{\mathrm{SL}}^{(1,\alpha)}(0)=4\sigma_X^2N_{\mathrm{SL}}(0)^2>0$, the last inequality in (refeq:65) means that all the relative maxima and minima of $F_{\mathrm{SL}}^{(mse)}(\alpha)$ occur when $F_{\mathrm{SL}}^{(mse)}(\alpha)$ is below the angle bisector α, as shown in Fig. 10. Thus, necessarily $F_{\mathrm{SL}}^{(mse)}(\alpha)$ crosses the angle bisector at least once, before its first relative maximum. Actually, to prove the uniqueness of such an intersection and, consequently, the uniqueness of the fixed point solution, it would be sufficient (not necessary) to prove that $F_{\mathrm{SL}}^{(mse)}(\alpha)$ is a contraction mapping [21] between the fixed point solution and its first relative maximum (e.g., $|F_{\mathrm{SL}}^{1,\alpha}(\alpha)|<1$ for $\alpha_{opt}<\alpha<\alpha_1^*$), as illustrated for more clarity in Fig. 10. Although it is not easy to analytically prove this inequality, it has been verified by brute force computer tests, partially reported in Fig. 14 , that it is always satisfied by any parameter set $\{A,\, T,\, \sigma_X\}$ and any SNR value, and, consequently, it is conjecture as true.

APPENDIX C

BNE DERIVATION

By observing (20), it is possible to proceed with the same approach of Appendix B. Due to the fact that (20) is a piecewise constant function with respect to $\alpha \in \mathcal{R}^+$, with a discontinuity in $\alpha = |x+n|$, the Dirac's impulse function $\delta(x)$ can be exploited to handle the derivative in such a point of the BN characteristic. Thus, by differentiating with respect to α, it is obtained that

$$\begin{aligned} h_{BN}^{(1,\alpha)}(x,n;\alpha) &= \tfrac{\partial h_{BN}(x,n;\alpha)}{\partial \alpha} \\ &= [h_{|n+x|^+}(x,n) - h_{|n+x|^-}(x,n)]\delta(\alpha - |n+x|) \\ &= -(n+x)\delta(\alpha - |n+x|), \end{aligned} \tag{66}$$

where $h_{a^\pm}(x,n) = \lim\limits_{\alpha \to a^\pm} h_{BN}(x,n;\alpha)$ represents the limit from either the right (+) or the left (−). Consequently, by direct substitution of (66)

$$\begin{aligned} h_\alpha(x,n;\alpha)h^{(1,\alpha)}(x,n;\alpha) &= -(n+x)h(x,n;\alpha)\delta(\alpha - |n+x|) \\ &= -(n+x)\tfrac{h_{|n+x|^+}(x,n)+h_{|n+x|^-}(x,n)}{2}\delta(\alpha - |n+x|) \\ &= -(n+x)\tfrac{x+(-n)}{2}\delta(\alpha - |n+x|) \\ &= \tfrac{(n^2-x^2)}{2}\delta(\alpha - |n+x|). \end{aligned}$$

By exploiting the equivalent expression of (17) for the BN, the optimum α, in the MMSE sense, is obtained as the solution of

$$\int_{-\infty}^{+\infty}\int_{-\infty}^{+\infty} (n^2 - x^2) f_X(x) f_N(n) \delta(\alpha - |x+n|) dx dn = 0,$$

which can be rewritten as

$$\int_{-\infty}^{+\infty}\int_{-\infty}^{-n} (n^2 - x^2) f_X(x) f_N(n) \delta(\alpha + x + n) dx dn + \int_{-\infty}^{+\infty}\int_{-n}^{+\infty} (n^2 - x^2) f_X(x) f_N(n) \delta(\alpha - x - n) dx dn = 0.$$

By exploiting the integral properties of the Dirac's delta functions, it is possible to recognize that

$$\int_{-\infty}^{+\infty} [n^2 - (-n-\alpha)^2] f_X(-n-\alpha) f_N(n) dn + \int_{-\infty}^{+\infty} [n^2 - (\alpha - n)^2] f_X(\alpha - n) f_N(n) dn = 0,$$

which, by simple manipulations, and exploiting the even symmetry of $f_X(x)$, can be simplified to

$$\alpha \int_{-\infty}^{+\infty} f_N(n) f_X(n+\alpha) dn = \int_{-\infty}^{+\infty} n f_N(n)[f_X(\alpha - n) - f_X(\alpha + n)] dn. \tag{67}$$

By substituting (3) in (67), the solution of the previous equation can be expressed as the solution to the fixed-point problem

$$\alpha = \frac{\sum\limits_{m=0}^{\infty} \beta_m \int\limits_{-\infty}^{+\infty} n f_m(n)[f_X(\alpha - n) - f_X(\alpha + n)]dn}{\sum\limits_{m=0}^{\infty} \beta_m \int\limits_{-\infty}^{+\infty} f_m(n) f_X(n + \alpha)dn}, \tag{68}$$

where the integral at the denominator is the convolution of two Gaussian, zero-mean *pdf*s, which generates another Gaussian *pdf* with a variance equal to the sum of the two variances. Consequently,

$$\alpha = \frac{\sum\limits_{m=0}^{\infty} \beta_m \int\limits_{-\infty}^{+\infty} n f_m(n)[f_X(\alpha - n) - f_X(\alpha + n)]dn}{\sum\limits_{m=0}^{\infty} \frac{\beta_m}{\sqrt{2\pi(\sigma_m^2 + \sigma_X^2)}} e^{-\alpha^2/2(\sigma_m^2 + \sigma_X^2)}}, \tag{69}$$

where the integral at the numerator can be split as the difference of a convolution and a correlation integral. By defining for convenience the odd function $p_m(n) = n f_m(n)$, it can be observed that

$$\begin{aligned} N_{\text{BN}}(\alpha) &= \int\limits_{-\infty}^{+\infty} n f_m(n)[f_X(\alpha - n) - f_X(\alpha + n)]dn \\ &= g_m(\alpha) * f_X(a) - g_m(-\alpha) * f_X(\alpha) \\ &= 2 g_m(\alpha) * f_X(\alpha) \\ &= 2\mathcal{F}^{-1}\{G_m(f) F_X(f)\}. \end{aligned} \tag{70}$$

By the same arguments that lead to equation (56) in Appendix A, (70) becomes,

$$N_{\text{BN}}(\alpha) = \frac{2\sigma_m^2}{\sqrt{2\pi}(\sigma_m^2 + \sigma_X^2)^{3/2}} \alpha e^{-\alpha^2/2(\sigma_m^2 + \sigma_X^2)},$$

and, consequently, the fixed-point equation is expressed by

$$\alpha = F_{\text{BN}}^{(mse)}(\alpha) = \frac{\sum\limits_{m=0}^{\infty} \frac{2\sigma_m^2 \beta_m}{(\sigma_m^2 + \sigma_X^2)^{3/2}} \alpha e^{-\alpha^2/2(\sigma_m^2 + \sigma_X^2)}}{\sum\limits_{m=0}^{\infty} \frac{\beta_m}{(\sigma_m^2 + \sigma_X^2)^{1/2}} e^{-\alpha^2/2(\sigma_m^2 + \sigma_X^2)}}, \tag{71}$$

which coincides with (21).

In order to prove the existence of the solution to the fixed point equation (71), first note that the problem has a different behavior with respect to the SLE case: indeed, $F_{\text{BN}}(\alpha)$ is monotonically increasing, as proved in the following. Lets for convenience express $F_{\text{BN}}(\alpha)$ in (71), by obvious notation equivalence,

$$F_{\text{BN}}^{(mse)}(\alpha) = \alpha G(\alpha) = \alpha \frac{N_G(\alpha)}{D_G(\alpha)} = \alpha \frac{\sum\limits_{m=0}^{\infty} a_m e^{-\alpha^2/2k_m}}{\sum\limits_{m=0}^{\infty} b_m e^{-\alpha^2/2k_m}}, \tag{72}$$

and its first derivative by

$$F_{\text{BN}}^{(1,\alpha)}(\alpha) = G(\alpha) + \alpha G^{(1,\alpha)}(\alpha), \tag{73}$$

where $G(\alpha) > 0$ for any α. Thus, in order to prove $F_{\text{BN}}^{(mse)}(\alpha)$ is monotonic, it is only requested to prove that $G^{(1,\alpha)}(\alpha) \geq 0$ for any α. To this end, lets express $G^{(1,\alpha)}(\alpha)$ as

$$\begin{aligned} G^{(1,\alpha)}(\alpha) &= \tfrac{1}{D_G^2(\alpha)} \left[N_G^{(1,\alpha)}(\alpha) D_G(\alpha) - N_G(\alpha) D_G^{(1,\alpha)}(\alpha) \right] \\ &= \tfrac{\alpha}{D_G^2(\alpha)} \sum_{m=0}^{\infty} \sum_{l=0}^{\infty} \tfrac{b_m a_l - a_m b_l}{k_m} e^{-\frac{\alpha^2}{2}\left(\frac{1}{k_m}+\frac{1}{k_l}\right)}, \end{aligned} \tag{74}$$

and note that the terms for $m = l$ null out in the double series in (74). Thus, due to the symmetry when the index m is interchanged with l, equation (74) can be rearranged as

$$G^{(1,\alpha)}(\alpha) = \frac{\alpha}{D_G^2(\alpha)} \sum_{m=0}^{\infty} \sum_{l=m+1}^{\infty} \left(\frac{b_m a_l - a_m b_l}{k_m} + \frac{b_l a_m - a_l b_m}{k_l} \right) e^{-\frac{\alpha^2}{2}\left(\frac{1}{k_m}+\frac{1}{k_l}\right)}. \tag{75}$$

By substituting in (75) the value of a_m, b_m, and k_m subsumed in (71) and (72), it is readily derived that

$$G^{(1,\alpha)}(\alpha) = \frac{2\alpha}{D_G^2(\alpha)} \sum_{m=0}^{\infty} \sum_{l=m+1}^{\infty} \frac{\beta_m \beta_j \sigma_X^2}{k_m^{5/2} k_l^{5/2}} \left(\sigma_m^2 - \sigma_l^2 \right)^2 e^{-\frac{\alpha^2}{2}\left(\frac{1}{k_m}+\frac{1}{k_l}\right)} \geq 0,$$

due to the fact that all the terms inside the double series are greater than zero. Thus, it is proved that $F_{\text{BN}}^{(mse)}(\alpha)$ is monotonically increasing, and that it starts from the non acceptable fixed-point solution $F_{\text{BN}}^{(mse)}(0) = 0$; additionally, by observing that $\sigma_m^2 = m\sigma_I^2/A + \sigma_I^2 \underset{m\to\infty}{\rightarrow} \infty$, it is proved that asymptotically$F_{\text{BN}}^{(mse)}(\alpha) > \alpha$, as verified by

$$\lim_{\alpha\to\infty} \frac{F_{\text{BN}}^{(mse)}(\alpha)}{\alpha} = \lim_{\alpha\to\infty} \frac{\sum\limits_{m=0}^{\infty} a_m e^{-\alpha^2/2(\sigma_m^2+\sigma_X^2)}}{\sum\limits_{m=0}^{\infty} a_m e^{-\alpha^2/2(\sigma_m^2+\sigma_X^2)}} = \lim_{\alpha\to\infty} \frac{a_\infty e^{-\alpha^2/2(\sigma_\infty^2+\sigma_X^2)}}{b_\infty e^{-\alpha^2/2(\sigma_\infty^2+\sigma_X^2)}} = \frac{2\sigma_\infty^2(\sigma_\infty^2+\sigma_X^2)^{1/2}}{(\sigma_\infty^2+\sigma_X^2)^{3/2}} = 2. \tag{76}$$

It is also highlighted, without a detailed proof, that $F_{\text{BN}}^{(mse)}(\alpha)$ starts to grow slower than α from $\alpha = 0$, as expressed by $F_{\text{BN}}^{(1,\alpha)}(0) = G(0) < 1$. Thus, (see Fig. 15) it is guaranteed that a solution (at least) exist for the fixed point problem. Moreover, with the support of extensive simulation trials (see Fig. 16) , it is reasonable to conjecture, that the fixed point problem for the BN has always the structure shown in Fig. 13. This conjecture guarantees the uniqueness of the (non-trivial) solution to the fixed-pint problem. Note that, the trivial solution $\alpha = 0$ should be avoided as starting point of the iterative algorithm A2.

REFERENCES

[1] D. Middleton, “Statistical-physical models of urban radio-noise environments - part i: Foundations,” *IEEE Trans. Electromagn. Compat.*, vol. EMC-14, no. 2, pp. 38–56 –, May 1972.

[2] ——, “Statistical-physical models of electromagnetic interference,” *IEEE Trans. Electromagn. Compat.*, vol. EMC-19, no. 3, pp. 106–127, Aug 1977.

[3] ——, “Canonical and quasi-canonical probability models of class a interference,” *IEEE Trans. Electromagn. Compat.*, vol. EMC-25, no. 2, pp. 76–106, May 1983.

[4] ——, “Non-gaussian noise models in signal processing for telecommunications: New methods and results for class a and class b noise models,” *IEEE Trans. Inf. Theory*, vol. 45, no. 4, pp. 1129–1149, May 1999.

[5] L. Berry, “Understanding middleton’s canonical formula for class a noise,” *IEEE Trans. Electromagn. Compat.*, vol. EMC-23, no. 4, pp. 337–344, Nov 1981.

[6] D. Middleton, “Procedures for determining the parameters of the first-order canonical models of class a and class b electromagnetic interference [10],” *IEEE Trans. Electromagn. Compat.*, vol. EMC-21, no. 3, pp. 190–208, Aug 1979.

[7] S. Zabin and H. Poor, “Parameter estimation for middleton class a interference processes,” *IEEE Trans. Commun.*, vol. 37, no. 10, pp. 1042–1051, 1989.

[8] ——, “Efficient estimation of class a noise parameters via the em algorithm,” *IEEE Trans. Inf. Theory*, vol. 37, no. 1, pp. 60–72, 1991.

[9] K. Blackard, T. Rappaport, and C. Bostian, “Measurements and models of radio frequency impulsive noise for indoor wireless communications,” *IEEE J. Sel. Areas Commun.*, vol. 11, no. 7, pp. 991–1001, 1993.

[10] Y.-Z. Jiang, X. lin Hu, X. Kai, and Z. Qi, “Bayesian estimation of class a noise parameters with hidden channel states,” in *Proc. IEEE Int. Symp. on Power Line Comm. and its Appl.(ISPLC’07)*, march 2007, pp. 2 –4.

[11] S. Rappaport and L. Kurz, “An optimal nonlinear detector for digital data transmission through non-gaussian channels,” *IEEE Trans. Commun.*, vol. 14, no. 3, pp. 266–274, Jun 1966.

[12] A. Spaulding and D. Middleton, “Optimum reception in an impulsive interference environment–part i: Coherent detection,” *IEEE Trans. Commun.*, vol. 25, no. 9, pp. 910–923, Sep 1977.

[13] A. Spaulding, “Locally optimum and suboptimum detector performance in a non-gaussian interference environment,” *IEEE Trans. Commun.*, vol. 33, no. 6, pp. 509–517, Jun 1985.

[14] D. Middleton, “Threshold detection in correlated non-gaussian noise fields,” *IEEE Trans. Inf. Theory*, vol. 41, no. 4, pp. 976–1000, Jul 1995.

[15] D. Stein, “Detection of random signals in gaussian mixture noise,” *IEEE Trans. Inf. Theory*, vol. 41, no. 6, pp. 1788–1801, 1995.

[16] A. Maras, “Adaptive nonparametric locally optimum bayes detection in additive non-gaussian noise,” *IEEE Trans. Inf. Theory*, vol. 49, no. 1, pp. 204–220, Jan 2003.

[17] A. Papoulis, *Probability, Random Variables, and Stochastic Processes*. McGraw-Hill, 1991.

[18] P. Kyees, R. McConnell, and K. Sistanizadeh, “Adsl: a new twisted-pair access to the information highway,” *IEEE Commun. Mag.*, vol. 33, no. 4, pp. 52–60, Apr 1995.

[19] K. Fazel and S. Kaiser, *Multi-carrier and spread spectrum systems:From OFDM and MC-CDMA to LTE and WiMAX*. Wiley Online Library, 2008.

[20] S. Zhidkov, “Performance analysis and optimization of ofdm receiver with blanking nonlinearity in impulsive noise environment,” *IEEE Trans. Veh. Technol.*, vol. 55, no. 1, pp. 234–242, Jan 2006.

[21] E. Süli and D. Mayers, *An introduction to numerical analysis*. Cambridge Univ Pr, 2003.

[22] H. E. Rowe, "Memoryless nonlinearities with gaussian inputs: Elementary results," *Bell Syst. Tech. J.*, vol. 61, no. 7, pp. 1519–1525, Sep 1982.

[23] S. Zhidkov, "Analysis and comparison of several simple impulsive noise mitigation schemes for ofdm receivers," *IEEE Trans. Commun.*, vol. 56, no. 1, pp. 5–9, Jan 2008.

[24] D. Guo, S. Shamai (Shitz), and S. Verd, "Mutual information and minimum mean-square error in gaussian channels," *IEEE Trans. Inf. Theory*, vol. 51, no. 4, pp. 1261–1283, Apr 2005.

[25] S. M. Kay, *Fundamentals of Statistical Signal Processing. Vol. 1, Estimation Theory*. Prentice-Hall, 1993.

[26] P. Banelli, "Another useful theorem for non-linear transformations of gaussian random variables," *in preparation*, vol. arXiv:1111.5950v1 draft version, pp. 1 –7, November 2011. [Online]. Available: http://arxiv.org/abs/1111.5950

[27] J. J. Bussgang, "Crosscorrelation functions of amplitude-distorted gaussian signals," *M.I.T. RLE Technical Report*, no. 216, pp. 1 –14, march 1952. [Online]. Available: http://hdl.handle.net/1721.1/4847

[28] R. Baum, "The correlation function of smoothly limited guassian noise," *IRE Trans. Inf. Theory*, vol. IT-3, pp. 193–197, Sep 1957.

[29] W. B. Davenport Jr. and W. L. Root, *An Introduction to the Theory of Random Signals and Noise*. Mc Graw Hill, 1958.

[30] P. Banelli and S. Cacopardi, "Theoretical analysis and performance of ofdm signals in nonlinear awgn channels," *IEEE Trans. Commun.*, vol. 48, no. 3, pp. 430–441, Mar 2000.

[31] K. Gulati, M. Nassar, A. Chopra, N. Ben Okafor, M. DeYoung, N. Aghasadeghi, A. Sujeeth, and B. L. Evans, *Interference Modeling and Mitigation Toolbox 1.6, for Matlab*, ESP Laboratory, ECE Dept., Univ. of Texas at Austin, Oct 2011.

[32] A. P. Prudnikov, Y. A. Brychkov, and O. I. Marichev, *Integrals and Series: Volume 2, Special Functions*. Gordon and Breach Science Publishers, 1986.

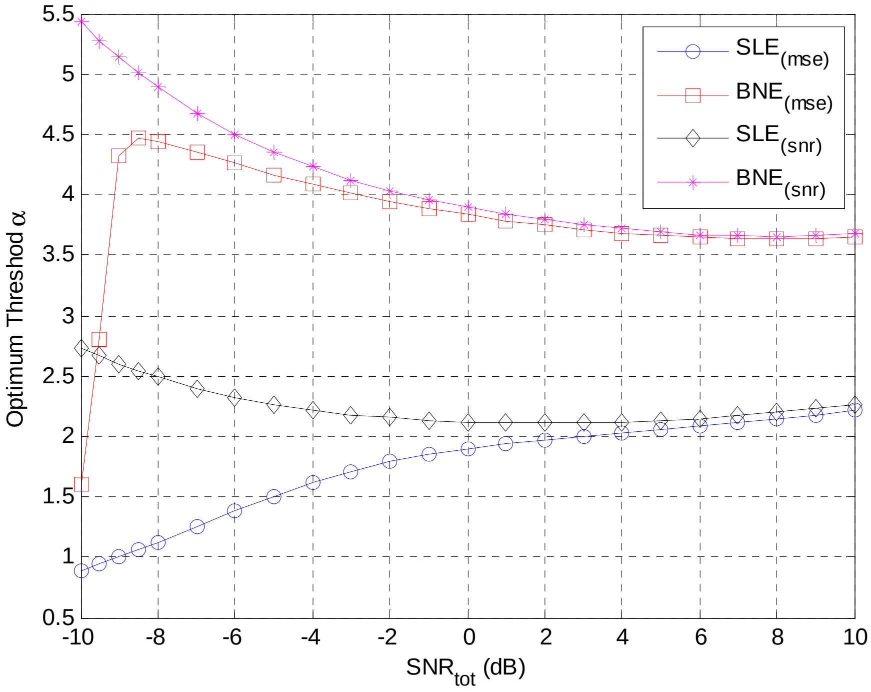

Fig. 5: Optimal SL and BN thresholds ($A = 0.01$, $T = 0.1$, $\sigma_X^2 = 1$)

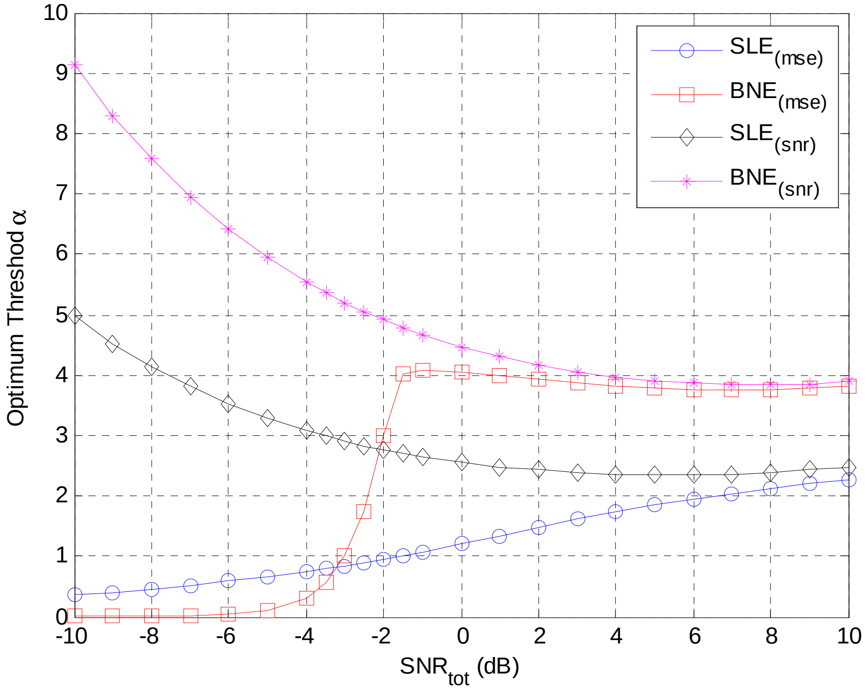

Fig. 6: Optimal SL and BN thresholds ($A = 0.01$, $T = 1$, $\sigma_X^2 = 1$).

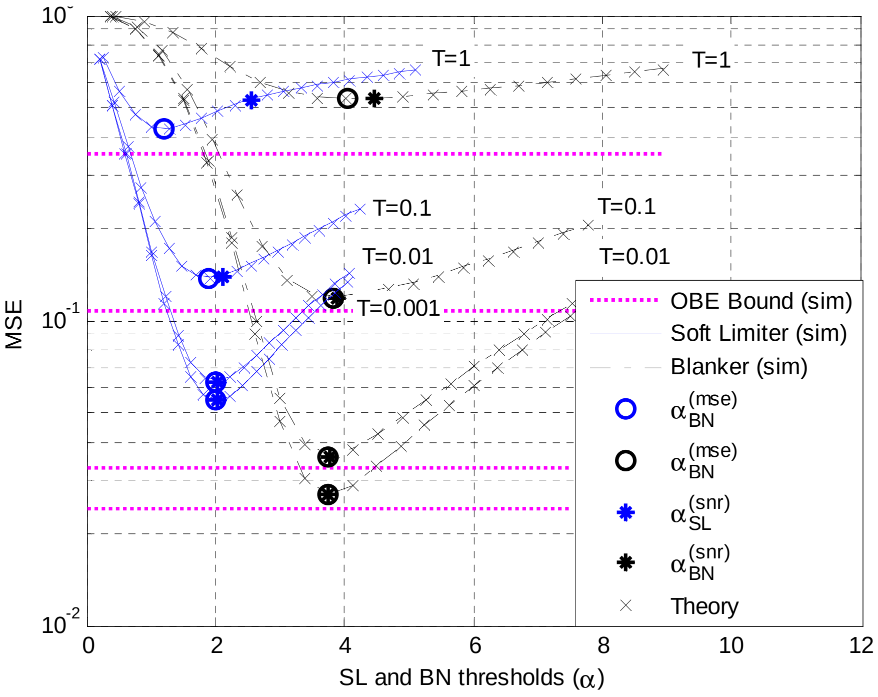

Fig. 7: MSE curves for $A = 0.01$ and $SNR_{tot} = 0$ dB

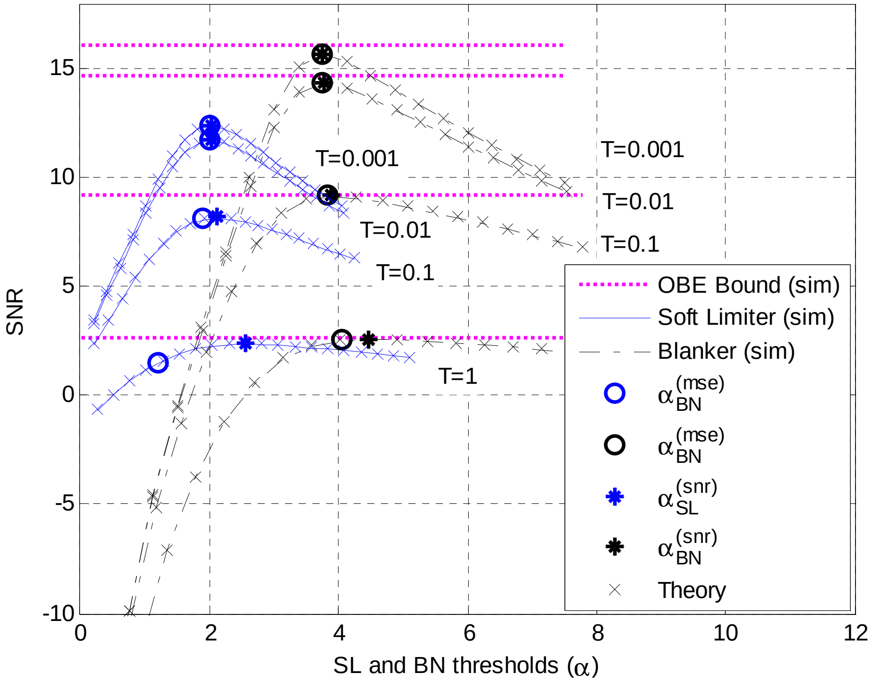

Fig. 8: SNR curves for $A = 0.01$ and $SNR_{tot} = 0$ dB

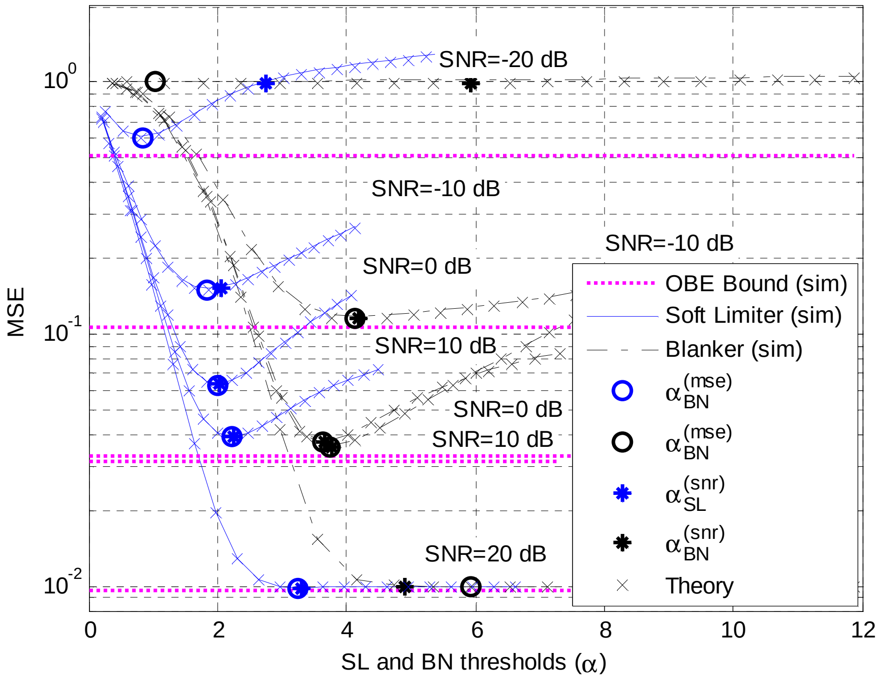

Fig. 9: MSE curves for $A = 0.01$ and $T = 0.01$

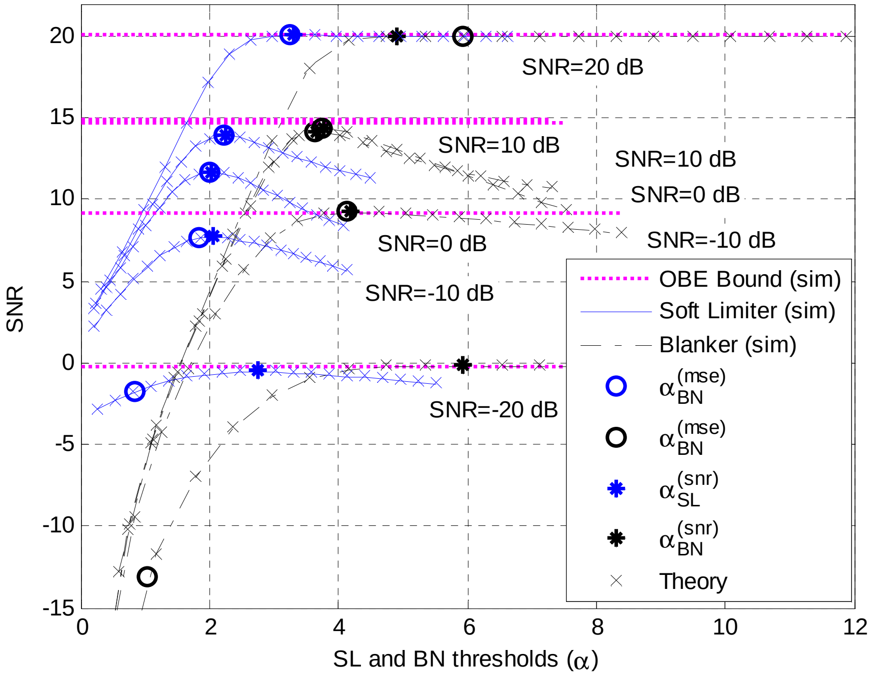

Fig. 10: SNR curves for $A = 0.01$ and $T = 0.01$

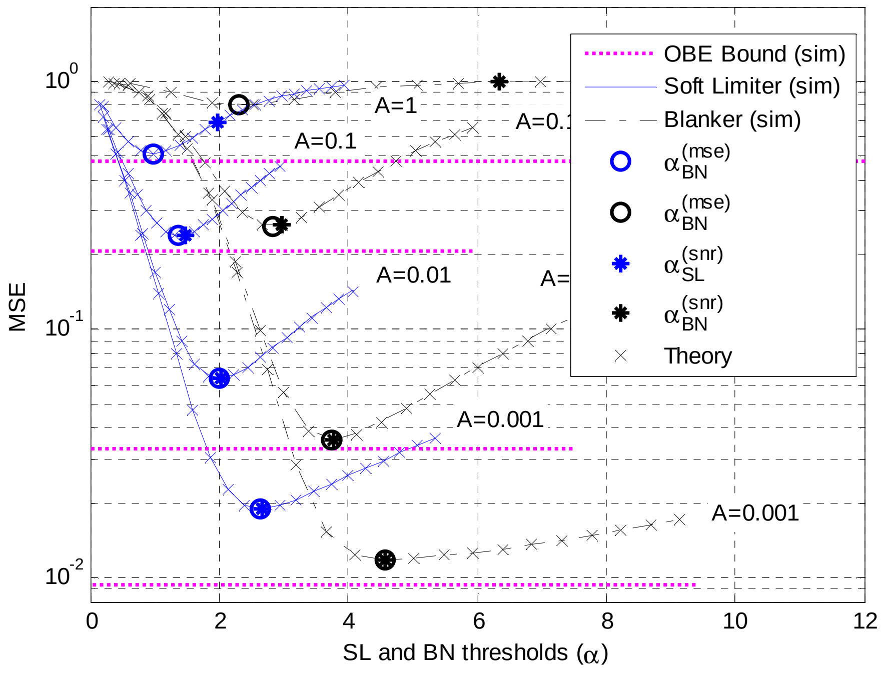

Fig. 11: MSE curves for $T = 0.001$ and $SNR_{tot} = 0$ dB

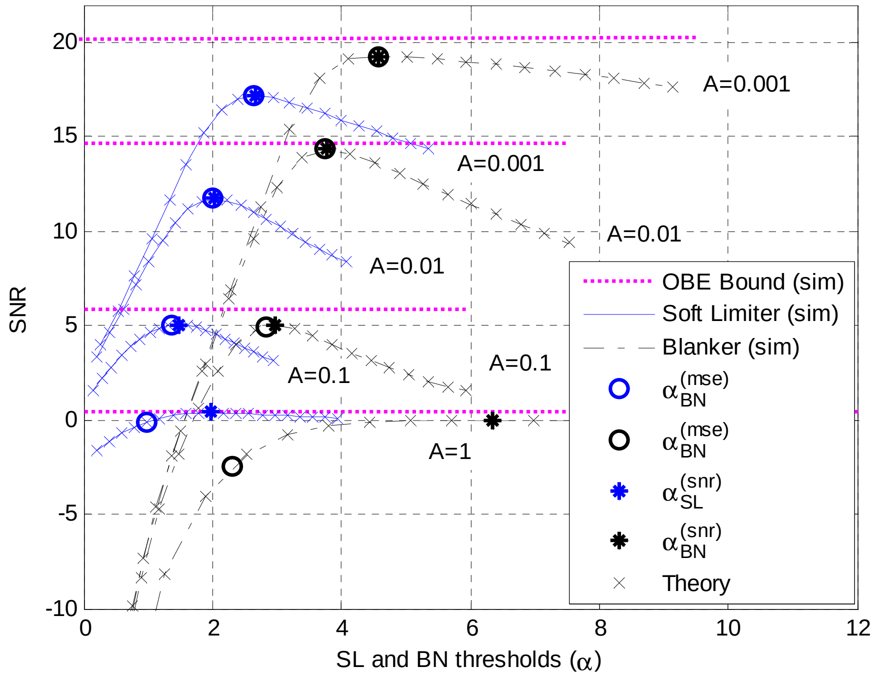

Fig. 12: SNR curves for $T = 0.001$ and $SNR_{tot} = 0$ dB

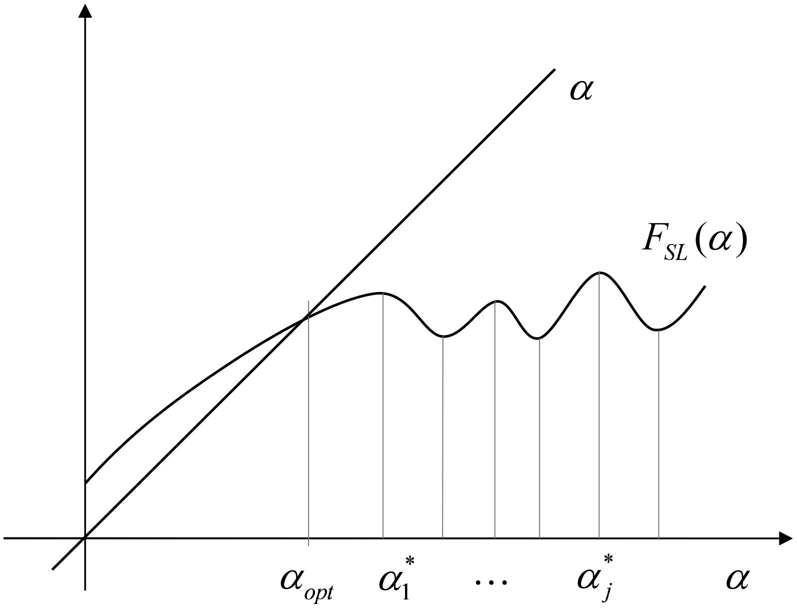

Fig. 13: Typical fixed point problem for the SLE

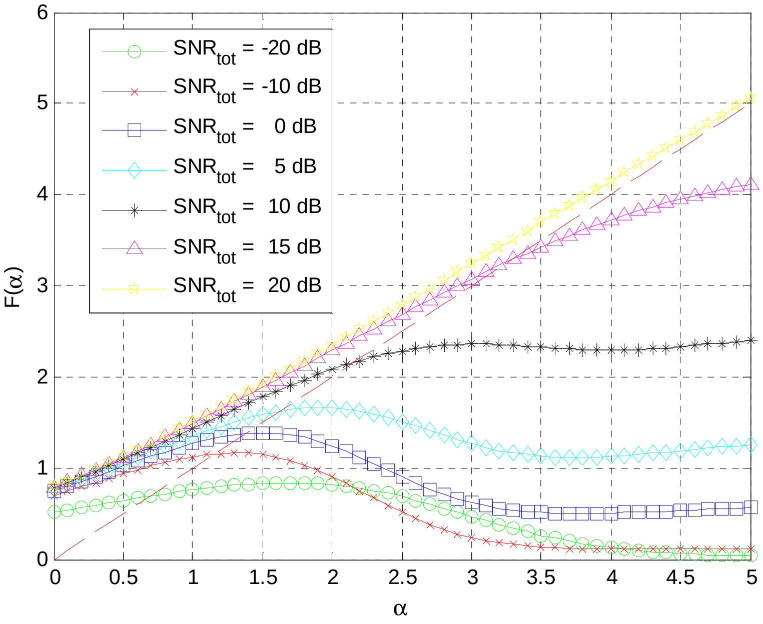

Fig. 14: Fixed point problem for the SLE, when $A = 0.1 \quad T = 0.01$, $\sigma_X^2 = 1$, for several values of the totalSNR.

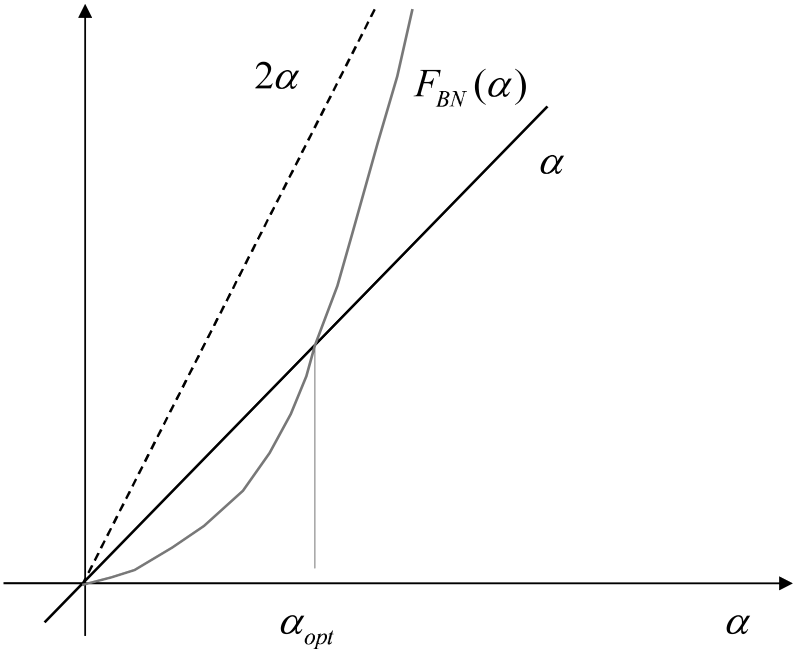

Fig. 15: Typical fixed point problem for the BNE

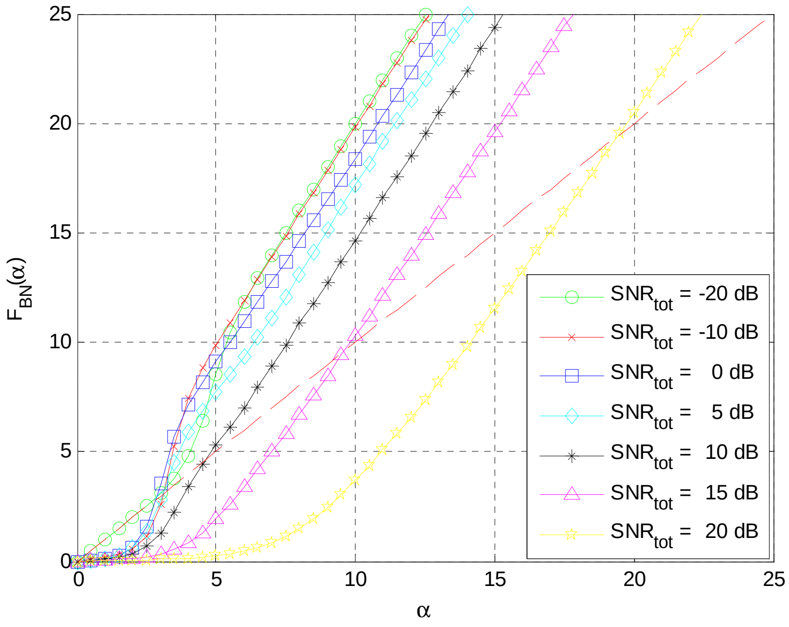

Fig. 16: Fixed point problem for the BNE, when $A = 0.1 \quad T = 0.01$, $\sigma_X^2 = 1$, for several values of the totalSNR.